

Validation of a 3D Velocity Model of the Puget Sound Region Based on Modeling Ground Motion from the 28 February 2001 Nisqually Earthquake

by Arben Pitarka, Robert Graves, and Paul Somerville

Abstract In this study we prepared a 3D velocity model suitable for modeling long-period wave propagation in the Puget Sound region. The model is based on products of the Seismic Hazard Investigation in Puget Sound (SHIPS) and geophysical information from other studies of the region. The adequacy of the velocity model was evaluated based on analyses of goodness of fit between recorded and simulated ground-motion velocity from the M 6.8 Nisqually earthquake. The earthquake was located about 60 km south of Seattle with a hypocentral depth of 59 km. The analyses were performed in the frequency range of 0.02–0.5 Hz, using data from 40 stations. Although our model covers a wide area of the Puget Sound region, its quality is assessed in the Seattle region in which the distribution of stations that recorded the Nisqually earthquake was denser. Our 3D finite-difference ground-motion modeling suggests that the propagation of long-period waves (periods longer than 3 sec) in the Seattle basin is mostly affected by the deep basin structure. The tomographic velocity model of Parsons *et al.* (2001), combined with the model of depth to the basement of the Seattle basin of Blakely *et al.* (1999), was essential in preparing and constraining geometrical features of the proposed velocity model.

Introduction

Important advances have been made in recent years regarding our understanding of the deep and shallow crustal structure in the Puget Sound region and its influence on ground shaking from recorded earthquakes and other seismic sources. Much of the knowledge has arisen from the SHIPS experiments (e.g., Brocher *et al.*, 1999; Brocher *et al.*, 2001; Parsons *et al.*, 2001; Calvert and Fisher, 2001; Van Wagoner *et al.*, 2002) and ground-motion analyses and modeling (e.g., Frankel *et al.*, 1999; Frankel and Stephenson, 2000; Hartzell *et al.*, 2000; Frankel *et al.*, 2002; Pratt *et al.*, 2003). Based on the SHIPS data, many comprehensive studies of the underground structure have provided valuable information that can improve the quality of existing crustal-velocity models that are used in strong ground-motion modeling and prediction in the Puget Sound metropolitan regions. The interpretation of refraction-survey data (e.g., Brocher *et al.*, 1999; Brocher *et al.*, 2001) and high-resolution tomographic models of the Seattle basin have provided new information about the geometry of the southern edge of the basin and the structure of the sedimentary layers. (e.g., Calvert and Fisher, 2001).

Investigations of geological structure in the Puget Sound metropolitan regions indicate the presence of strong lateral variations in the near-surface geology (e.g., Finn *et al.*, 1991; Johnson *et al.*, 1999; Pratt *et al.*, 1997; Brocher *et al.*, 2001; Calvert and Fisher, 2001). These basin struc-

tures have the potential to significantly increase the amplitude and duration of strong ground motions. Based on analyses of the site response by using ground motions from regional earthquakes, Frankel *et al.* (1999) found large amplification for sites on artificial fill and modified land in the central part of the Seattle basin. Using similar analyses but a larger data set, Hartzell *et al.* (2000) found that the large variability of the ground motion in the Seattle basin can be attributed not only to variations in the Quaternary deposits but also to 3D basin-structure effects. This was confirmed by 3D simulations of long-period ground motions in the Seattle region by using a finite-difference method performed by Frankel and Stephenson (2000). Amplified ground motion with increased duration could cause significant damage to the built environment in the Seattle area, even during moderate earthquakes. This is demonstrated by the magnitude 6.8 28 February 2001 Nisqually earthquake, which caused \$2 billion in damage. The development of 3D velocity models capable of accurately reproducing the effects of deep and shallow geology on ground motions from faults within the Puget Sound metropolitan regions is therefore an important task for seismic-hazard assessment. The work presented here describes our effort to develop a 3D velocity model of the Puget Sound region that incorporates recent information on the structure of the crust, especially in the Seattle region. We discuss the details of the model param-

terization and show results of the model validation analyses, using recorded ground motion from the 2001 Nisqually earthquake.

Velocity Model Parameterization

The extensive SHIPS geophysical experiment and other high-resolution surveys have helped to better characterize the crustal architecture and basin geometry, and to map the sediment thickness and location of fault zones, in the Puget Sound region. These investigations are summarized in Table 1. Tomographic velocity models of the Puget Sound region (e.g., Parsons *et al.*, 2001; Brocher *et al.*, 2001; Crosson, 1976; Van Wagoner *et al.*, 2003) are characterized by marked lateral variation of the velocity in the crust and the existence of deep basin structures. In order to provide accurate information on the effects of these underground-structure complexities on the ground motion from earthquakes in the region, we need to progressively improve our velocity models by modeling more ground-motion data as they become available and extend the modeling capability to high frequencies. By modeling higher frequencies we will be able to provide constraints that are crucial for solving ambiguities in the velocity models inherited from the generalization of limited geophysical and geotechnical information. The analysis of modeling presented here is a part of such efforts.

Based on results of some of the SHIPS investigations, we produced a 3D velocity model for an area that includes parts of the Puget Sound region. The location of the area covered by our model, and ground-motion-recording stations used in this study, are shown in Figure 1. Our velocity model occupies a volume of $61 \times 82 \times 62$ km and is characterized by three main components: (1) the background 3D crustal structure, (2) the basement and sedimentary layers

of the Seattle basin, and (3) the thickness of the unconsolidated deposits throughout the region. The 3D tomographic P -wave-velocity crustal model of Parsons *et al.* (2001) was used to generate the background velocity of our model which reaches a depth of 62 km. The Parsons *et al.* (2001) model was obtained by inverting combined dense seismic-reflection travel times and gravity-anomaly data. The model gives the P -wave velocity on a regular grid with a constant spacing of 1 km. We resampled it on a finer grid with variable vertical spacing. The velocity at each point of the refined grid was calculated by linearly interpolating the velocity corresponding to the eight closest grid points of the original grid. The S -wave velocities in our model were derived from the P -wave velocities by using the V_p/V_s ratio. Following Frankel and Stephenson (2000), the V_p/V_s ratio was assumed to be 2.2 and 1.75 at depths above 2.5 km and below 2.5 km, respectively, whereas the density increases from 2.3 gm/cm^3 to 2.7 gm/cm^3 . Another velocity-model parameter used in our wave-propagation finite-difference modeling method is the anelastic attenuation, which is represented by the Q factor. The implementation of the attenuation into our finite-difference method is based on the Graves (1996) technique, which considers Q to be the same for both P and S waves, and frequency independent. Because of the lack of reliable information on the anelastic attenuation in the considered region, we assumed Q to be 100 and 500 at depths smaller and greater than 2.5 km, respectively, except for the unconsolidated deposits, where Q was assumed to be 50.

The part of the model that includes the Seattle basin to a depth of 10 km was prepared by using combined data from the depth-to-basement map of Blakely *et al.* (1999) and a north-south cross section of the Seattle basin sediments based on the interpretation of seismic-reflection profiles during the SHIPS experiment (Brocher *et al.*, 2001). This velocity profile, and a high-resolution tomographic model of

Table 1
Recent Investigations of Crustal Structure in the Seattle Area Considered in This Study

Objective	Type of Data and Investigation	Product	References
Crustal Structure	Seismic-reflection travel-time tomography	3D tomography P -wave model	Brocher <i>et al.</i> (2001)
	Inversion of travel time and gravity data	3D tomography P -wave model	Parsons <i>et al.</i> (2001)
	Seismic reflection and seismicity, travel-time tomography	3D tomography P -wave model	Crosson (1976)
	Travel-time tomography	3D tomography P -wave model	Van Wagoner <i>et al.</i> (2002)
Shallow Crustal Structure	Inversion of gravity and aeromagnetic data	Depth to basement	Blakely <i>et al.</i> (1999)
	High-resolution seismic reflection	2D tomography P -wave model	Miller and Snelson (2001)
	High-resolution seismic reflection	2D tomography P -wave model	Calvert and Fisher (2001)
	Inversion of gravity data	Velocity structure 3D sedimentary-layer model	Pratt <i>et al.</i> (1997) Finn <i>et al.</i> (1991)
Quaternary Layer	Geotechnical investigations	Depth to bedrock, northern Puget Sound	Yount <i>et al.</i> (1985)
	Geotechnical investigations	Depth to bedrock, southern Puget Sound	Hall and Othberg (1974)
	Seismic-reflection and borehole data	Thickness of Quaternary deposits	Johnson <i>et al.</i> (1999)
Shallow Velocities	Borehole logging	Velocity and density	Brocher and Ruebel (1998)
	Shallow seismic refraction	Seismic velocity	Williams <i>et al.</i> (1999)
	Geotechnical and geophysical data	Shear-wave velocity	Wong <i>et al.</i> (1998) Silva <i>et al.</i> (1995)

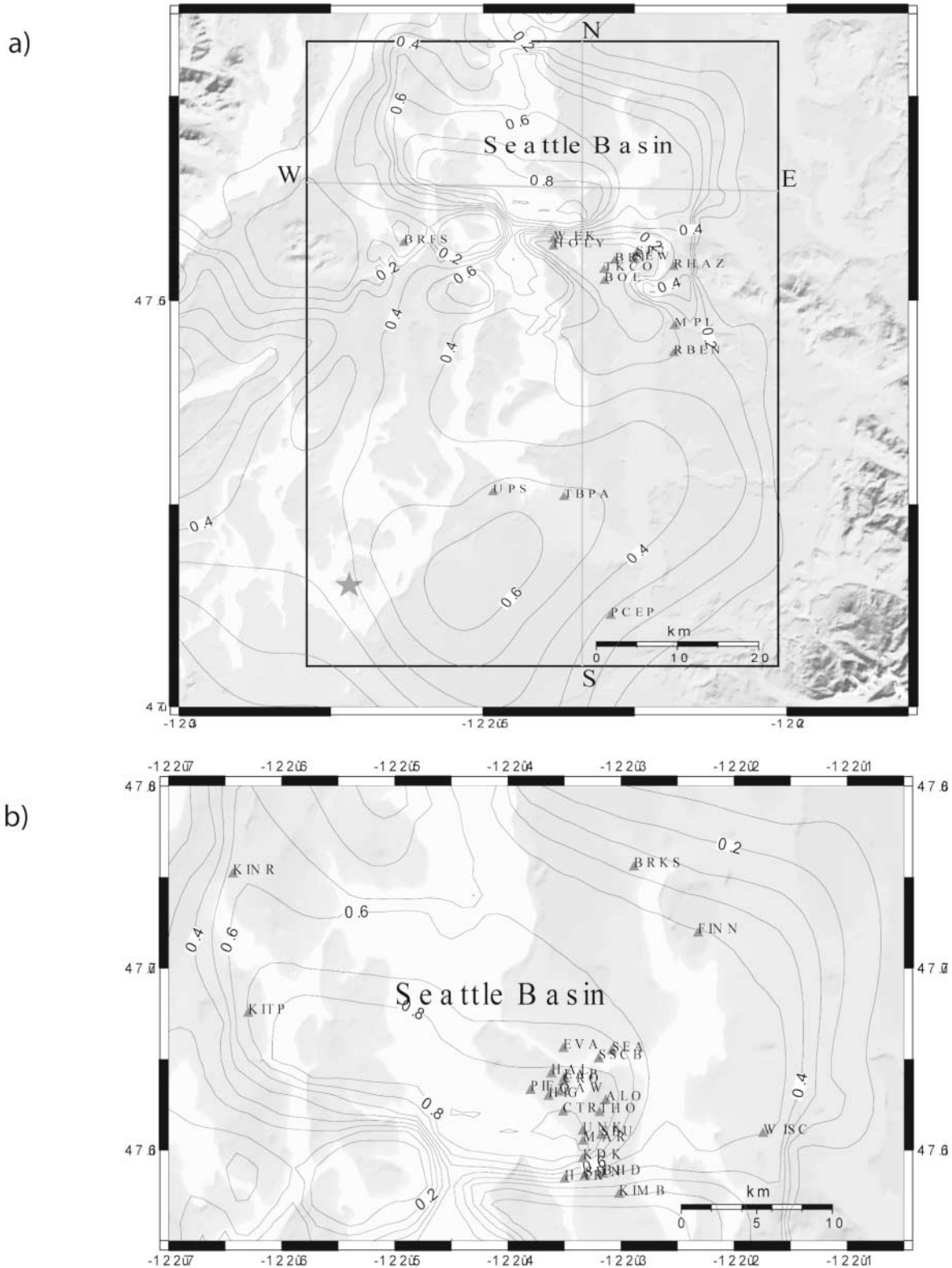


Figure 1. (a) Map of the Puget Sound area. (b) Map of the Seattle basin area. Black rectangle delineates the area covered by the 3D velocity model. Thin solid lines indicate the locations of north-south and east-west vertical cross sections of the model. Triangles show the locations of the strong-motion stations, and the star shows the epicenter location of the Nisqually earthquake. Contour lines represent the depth to the base of unconsolidated deposits.

the area, suggest that the southern edge of the Seattle basin dips toward the south. This important feature of the southern edge of the basin was not resolved by the gravimetric and aeromagnetic data used by Blakely *et al.* (1999) and is therefore not present in his depth-to-basin basement model. The profile, which extends to more than 10 km in depth, suggests that the basin sediments below 1 km consist of at least four distinctive layers with strong velocity contrast. In our model the profile was used to derive the geometry of the southern edge of the Seattle basin and the decreasing thickness of the sedimentary layers toward the north. The lateral variation of the thickness of the layers was assumed to be proportional to the corresponding basin depth, and its north–south variation was assumed to be similar to that of the north–south velocity profile (see Fig. 2). This procedure produces a basin velocity model that agrees with a 2D velocity model along an east–west cross section of the basin that was proposed by Miller and Snelson (2001). Their model indicates that the

geometry of the boundaries between the sedimentary layers is similar to that of the basin basement. The assumed seismic parameters of the sedimentary layers are given in Table 2.

Besides the Seattle basin structure, a key feature in our velocity model is the thickness of the layer representing the unconsolidated deposits, which consist mainly of Quater-

Table 2
Velocity Model of the Seattle Basin Sediments

Layer	V_p (km/sec)	V_s (km/sec)	Density (g/cm ³)	Q
Quaternary	1.5	0.6	2.1	50
1	1.8	1.2	2.2	50
2	2.7	1.6	2.4	50
3	3.3	1.9	2.6	250
4	4.0	2.3	2.7	300
5	5.3	3.1	2.8	400

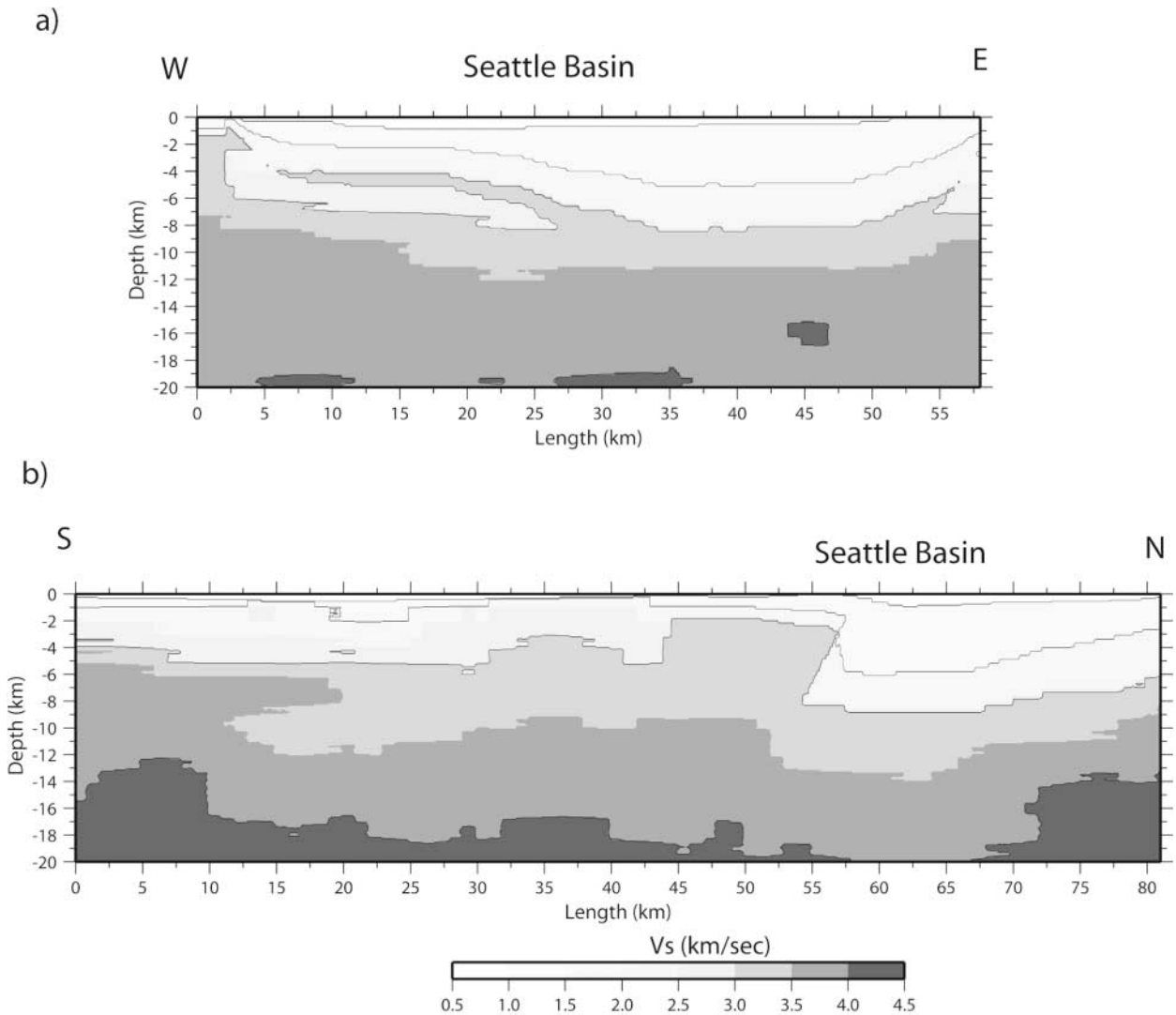


Figure 2. Upper 20 km of vertical cross sections of the 3D velocity model along the east–west and north–south profiles shown in Figure 1.

nary and possibly Pliocene deposits. The thickness of the unconsolidated deposits is well resolved only in the Seattle region where the surface deposits consist of Quaternary sediments (Johnson *et al.*, 1999). In the other areas of the Seattle region, our knowledge of the thickness of such deposits is poor. In our model it was derived from the maps of depth to basement of Yount *et al.* (1985) and Hall and Othberg (1974) for the northern part and the southern part of the Puget Sound region, respectively. These maps are based on geotechnical investigations, using extrapolations between data that are sparsely distributed. Most of the wells used to estimate the depth to basement do not penetrate to the base of the deposits, and hence the thickness of the unconsolidated sedimentary layer in our model is not well resolved. Other studies of the shallow seismic velocity of the unconsolidated deposits suggest that the shear-wave velocity increases rapidly with depth, with values as low as 150 km/sec at the surface (Wong *et al.*, 1998). The representation of small-scale variations of the unconsolidated sedimentary layer in our model would require a very fine grid with spacing on the order of 10 m. Because of its extremely large computational requirement, such a dense grid is not practical for wave-propagation modeling using available numerical techniques. In the velocity model we tested the minimum grid spacing is 200 m. Consequently, the unconsolidated deposits are represented by a single layer with a minimum shear-wave velocity of 0.6 km/sec. For this layer we assumed $V_p = 1.5$ km/sec, density = 2.1 g/cm³, and $Q = 50$.

Vertical cross sections of the 3D velocity model up to a depth of 20 km, oriented in the east–west and north–south directions across the Seattle basin, are shown in Figure 2a and b, respectively. The locations of the profiles are indicated by this solid lines in Figure 1a. The strong discontinuity in the geological structure caused by the Seattle fault created a zone of velocity contrast along the southern edge of the Seattle basin. The velocity contrast between the basement and the basin sediments, and the geometry of the basin edge in this area, are key features of the basin structure that generate secondary basin waves. As will be seen in the simulation results, these waves mostly affect the amplitude and duration of the ground motion at basin sites. The velocity structure below 20-km depth is very simple, consisting mainly of very small vertical variations in the velocity. The shear-wave velocity gradually increases from 4 to 4.57 km/sec in the depth interval of 20–62 km. This structure is consistent with the results from a recent study that shows clear evidence that the region considered here is underlain by a low-velocity, serpentinized upper mantle (Brocher *et al.*, 2003). The reduction of the velocity contrast in the Moho boundary caused by the low velocity in the upper mantle has significant effects in ground motions from deep earthquakes, such as the Nisqually earthquake, which may reduce the amplitude and duration of the ground motion.

Our model shares some similarities and dissimilarities with another velocity model of the Seattle basin area that was proposed by Frankel and Stephenson (2000). Both ve-

locity models use the same depth to the basin basement and the same data for the Quaternary layer. The main differences are in the way the basin sedimentary layers are represented, the geometry and dip angle of the southern edge of the basin, and the background regional velocity model.

Modeling Ground Motion from the 2001 Nisqually Earthquake

As a first step in the process of testing the velocity model, we computed long-period ground motion (2–10 sec) for the 28 February 2001 Nisqually earthquake (M 6.8) and compared the synthetic and recorded velocity seismograms at 40 strong-motion recording sites. The hypocenter was located at -122.4 E and 32.5 N at a depth of 59 km (Ichinose *et al.*, 2002). The earthquake was recorded by strong-ground-motion stations operated by the U.S. Geological Survey and the University of Washington. Because the earthquake source was relatively deep, most of the ground motion recorded at basin sites was dominated by direct shear waves and basin-generated secondary waves. The recordings of such waves, and the relatively dense station distribution in the Seattle basin, provided excellent information that was useful in analyzing the ability of the velocity model to reproduce the main characteristics of the observed ground motion, especially in the Seattle basin area.

The simulation was performed by using the finite-difference method of Pitarka (1999) using a regular grid with variable spacing in the vertical direction. The minimum grid spacing of 200 m and its vertical variation ensured accurate calculations of the wave field up to a frequency of 0.5 Hz. The earthquake source was modeled by two double-couple point sources separated in time by 1.5 sec. Our source model was derived from the slip model obtained by Ichinose *et al.* (unpublished manuscript), based on the inversion of ground motion and teleseismic data. The source model used in the finite-difference simulation is described in Table 3. The source time function for each point source was assumed to be of triangular shape.

The comparison between the synthetic- and recorded-velocity seismograms at sites inside and outside the Seattle basin, starting with the station closest to the epicenter, is shown in Figures 3 and 4, respectively. Both synthetic and recorded data are bandpass filtered at 0.1–0.5 Hz. The model does a good job of reproducing the phases carrying most of the seismic energy, and the duration of the ground motion at the Seattle basin sites. At sites HAR, SDN, KIMB, BHD, and KDK, near the southern edge of the basin, the waveform

Table 3
Point-Source Model of the Nisqually Earthquake

Point Source	Strike (°)	Dip (°)	Rake (°)	Depth (km)	Rise Time (sec)	M_0 (dyne cm)
1	356	68	-90	55.0	4.0	0.7×10^{26}
2	356	68	-100	55.0	4.5	1.1×10^{26}

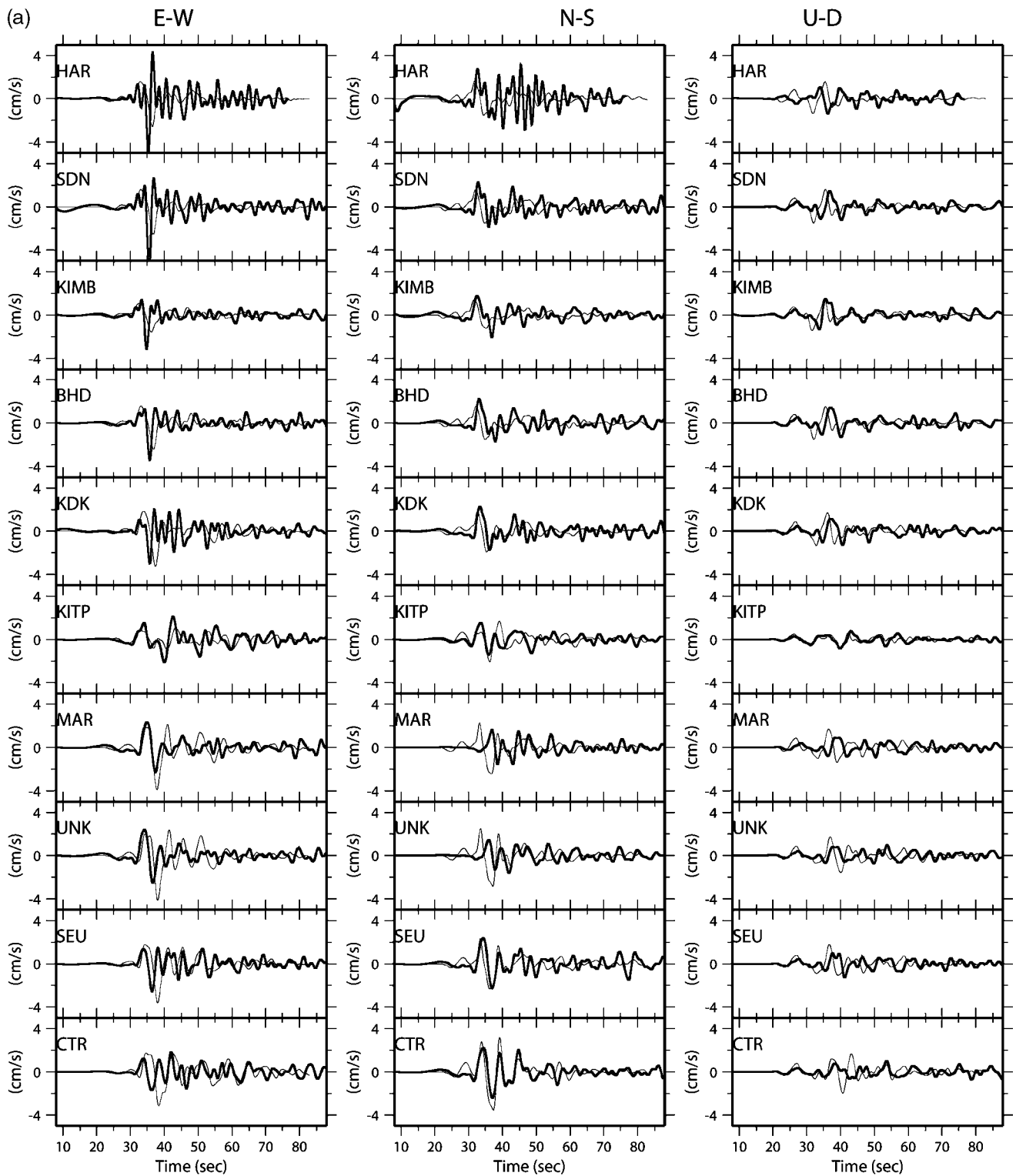


Figure 3. Caption on page 1677.

fit is less satisfactory. At these sites, scattered waves with periods shorter than 3 sec are less developed in the synthetic seismograms. Such waves consist of reverberations of waves trapped within the surface layers. The discrepancy may be

related to the minimum shear-wave velocity of 600 m/sec imposed to our model, which may alter wave-propagation effects within the surface layers. It is also possible that the absence of high-frequency waves in the synthetics is caused

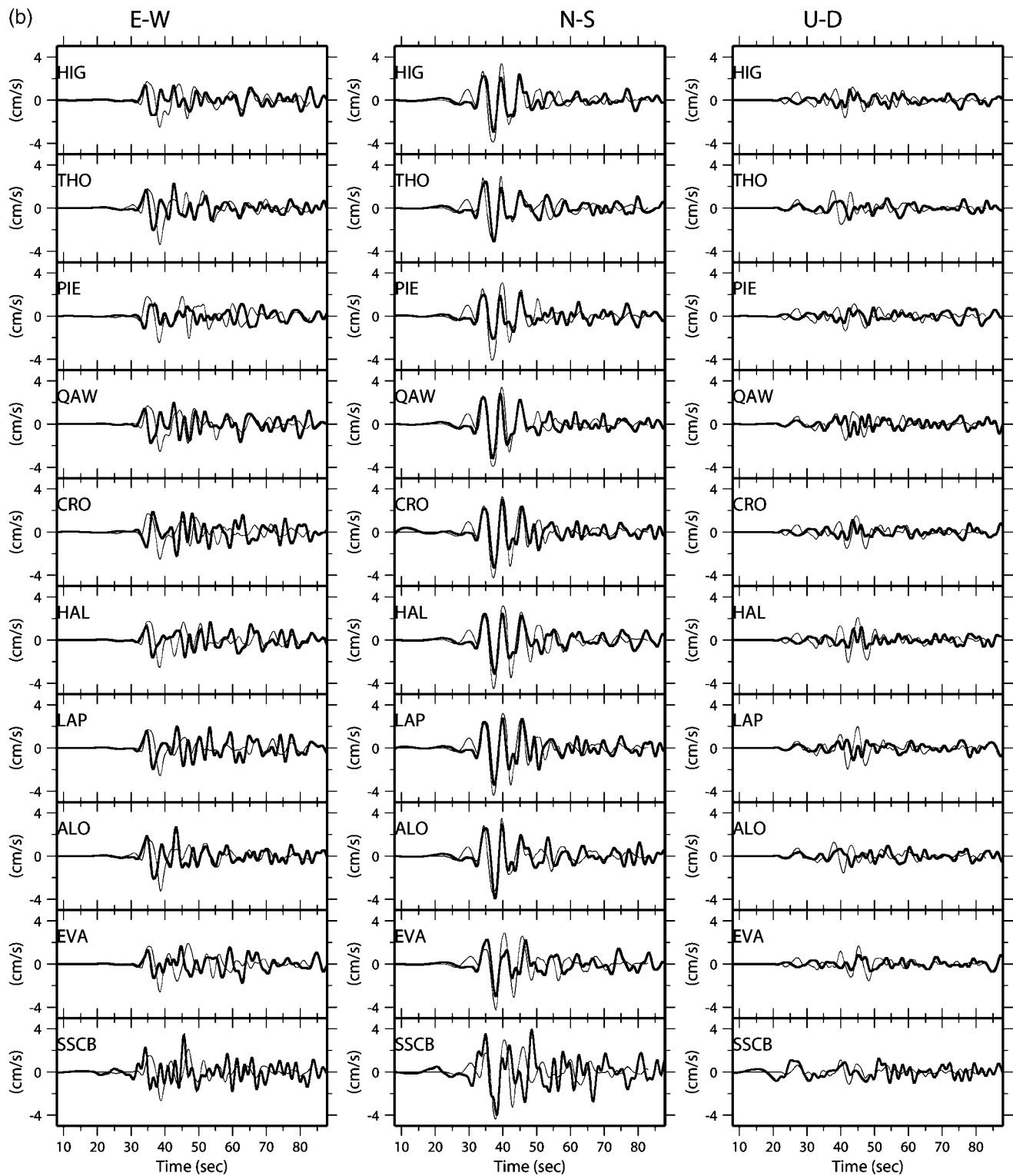


Figure 3. Caption on page 1677.

by the lack of high-frequency variation in our slip-velocity function, which has spectral holes of about 2–2.5 sec. At sites in the central part of the basin and near the Ship Canal (e.g., CTR, HIG, THO, QAW, ALO, EVA, and SEA) the wave-

form fit is relatively good. At these sites the ground motion is characterized by two long-period pulses followed by others with smaller amplitude. The first large pulse is the direct *S* wave. The other large pulse, following the first one,

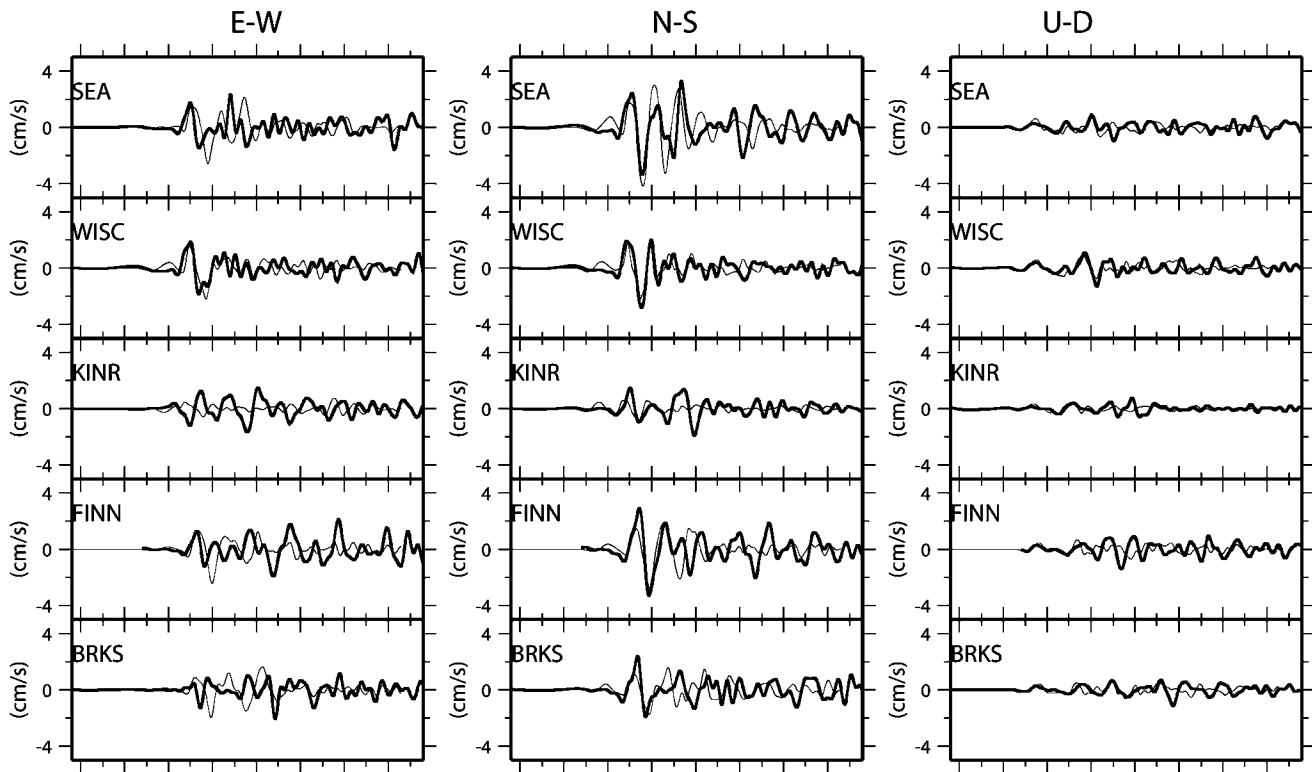


Figure 3. Comparison of recorded (thick line) with synthetic (thin line) velocity seismograms at sites in the Seattle basin.

is a basin basement-reflected wave, which is mainly polarized in the vertical plane. Its amplitude remains significant even at stations FINN and BRKS, where the shallow sedimentary layers become thinner, but the basement is still deep. Our simulation reproduces both pulses very well. A third phase, followed by coda waves, can be seen clearly in the east–west component of ground motion recorded at stations SEU, THO, PIE, QAW, CRO, HAL, ALO, EVA, and SSCB, which are north of the southern edge of the basin. At these sites this phase arrives at least 15 sec after the direct S wave. Its amplitude is comparable or even larger than that of the direct S wave, and the delay time increases from south to north. As will be seen in maps of simulated peak-velocity distribution, this phase dominates the peak velocity at sites around the Ship Canal in the central part of the basin. A similar phase was observed by Frankel and Stephenson (2000) in their simulation of a shallow M 5.0 earthquake on the Seattle fault, which bounds the southern edge of the basin. They describe it as a surface wave of higher mode, trapped in the Quaternary deposits and amplified by the thinning of the shallow deposits toward the north. Our simulation of the Nisqually earthquake, which was generated by a deep fault, indicates that such a phase may not be associated only with earthquakes on the Seattle fault.

At sites outside the basin the waveform fit between the recorded and simulated seismograms is good except for UPS, PCEP, and BRFS, which are in the southern part of the model in a deep basin. At these stations most of the seismic energy

is carried by coda waves with periods between 2 and 3 sec. The simulation reproduces only the first part of the seismograms. The extremely long duration of the recorded coda waves and their relatively high frequency, not reproduced by our model, indicate that the large basin structure in the southern part of the considered region is much more complex than the one in our model.

At sites in the southern and central parts of the Seattle basin, the travel time of the recorded largest pulse associated with the direct shear wave is shorter by at least 2 sec in the east–west component than in the north–south component (see recorded motion at BHD, KDK, MAR, UNK, SEU, QAW, CRO, ALO, EVA, and SEA, shown in Fig. 3). This phenomenon is not observed at sites outside the basin. The fact that this time delay is not reproduced by our model, in which the soil is considered as isotropic (compare the synthetic and observed seismograms at the stations mentioned above), suggests that anisotropy exists in the soil properties in the regions around the southern edge of the basin. This indicates that the Tertiary sedimentary rocks of the Seattle fault zone are highly fractured.

Goodness of Fit between Observed and Simulated Ground-Motion Velocity

In order to evaluate the quality of our velocity model, we analyzed the goodness of fit between simulated and recorded ground motion. Goodness-of-fit factors were derived

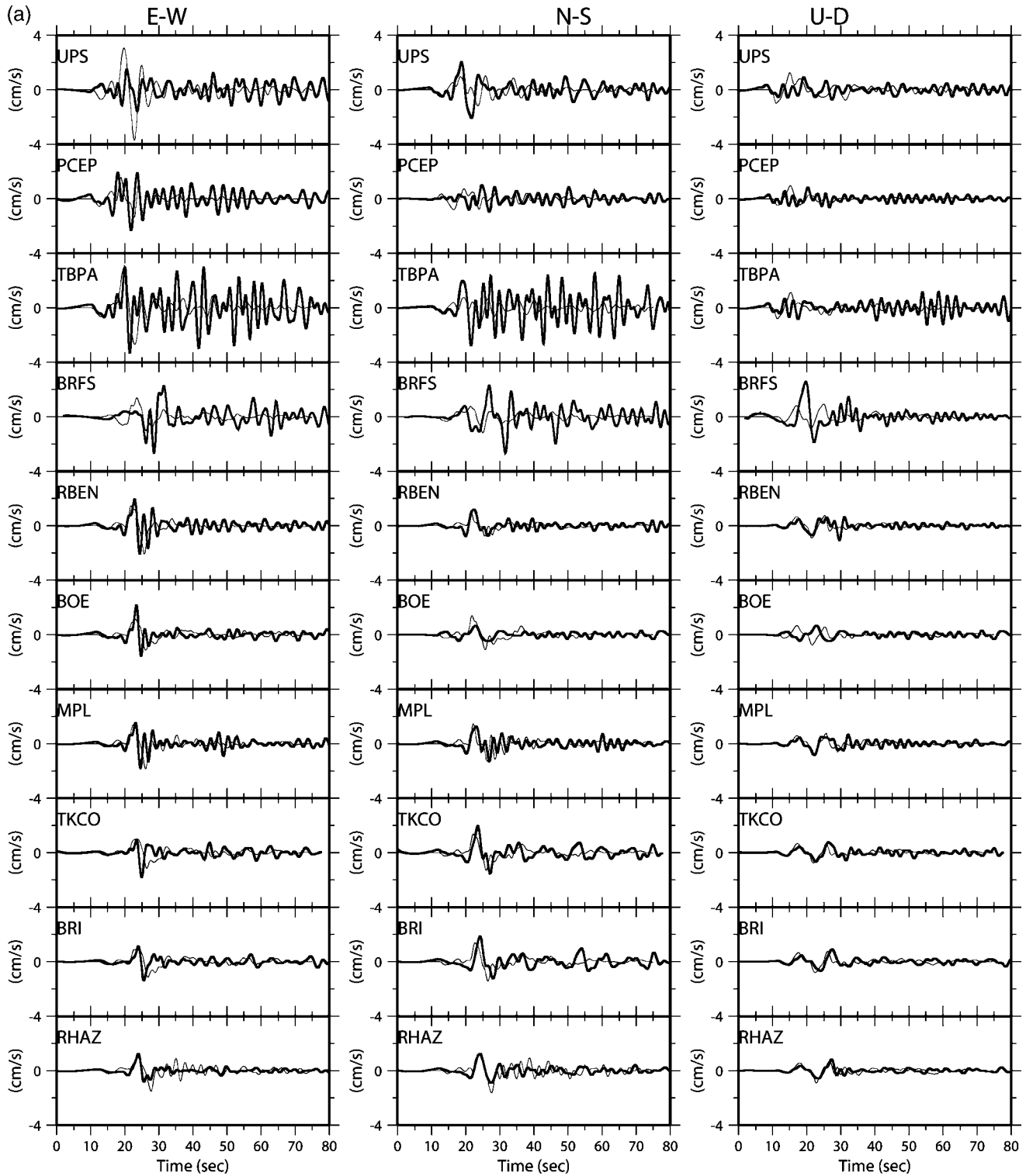


Figure 4. Caption on next page.

for different ground-motion parameters, such as peak velocity and Fourier amplitude spectra, in a given frequency range. The goodness-of-fit factor, f_1 , corresponding to a ground-motion parameter, is given by John Anderson (2003, personal comm.):

$$f_1 = \exp \left[- \left(\frac{\text{Syn} - \text{Obs}}{\min(\text{Syn}, \text{Obs})} \right)^2 \right],$$

where Obs and Syn are measures of the ground-motion parameter using observed and synthetic seismograms, respec-

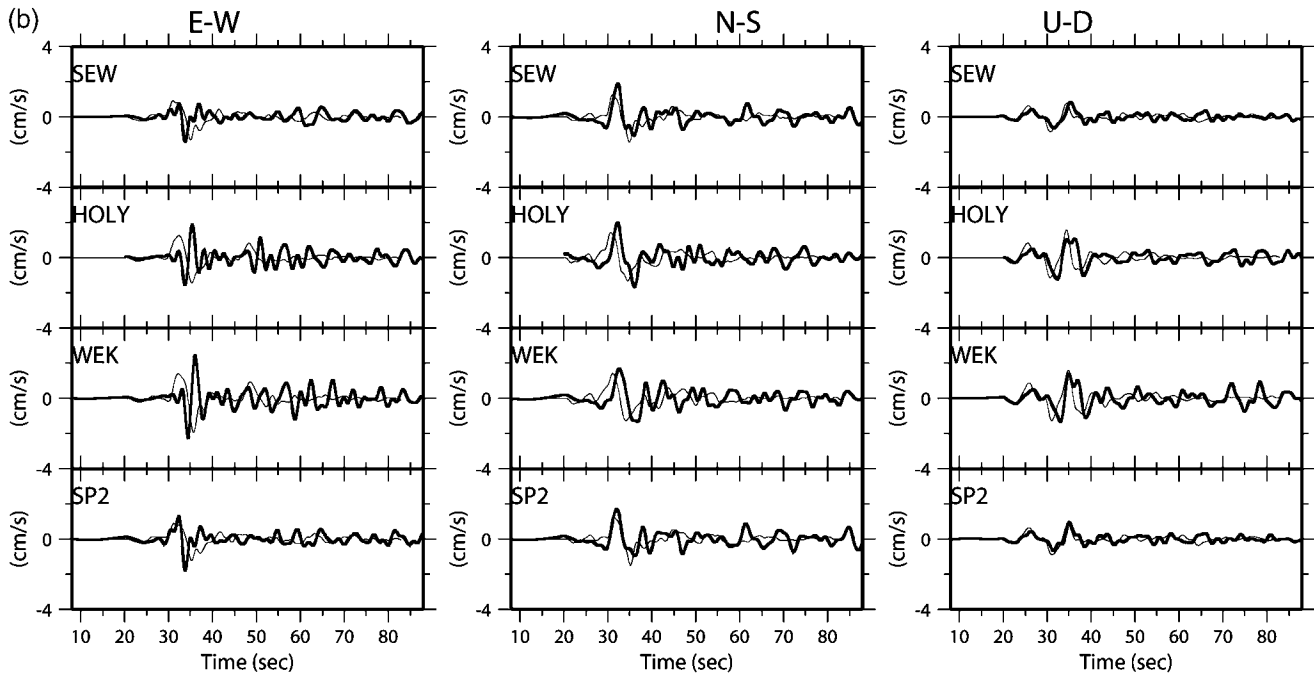


Figure 4. Comparison of recorded (thick line) with synthetic (thin line) velocity seismograms at sites outside the Seattle basin.

tively, and $\min(\text{Syn}, \text{Obs})$ is the smaller of the two; f_1 varies from 0 to 1, with 1 corresponding to identical observed and simulated ground-motion measures. In this study we calculated f_1 by using the peak ground velocity (PGV) of seismograms bandpass filtered at three different frequency ranges of 0.05–0.2 Hz, 0.05–0.3 Hz, and 0.05–0.5 Hz, respectively, and Fourier spectra amplitude (FSA) averaged over a narrow band of 0.1 Hz, centered at 0.2, 0.3, and 0.4 Hz.

In addition to f_1 , we calculated factor f_2 , which is given by the following formula:

$$f_2 = 2 \frac{\int p(t)_{\text{obs}} p(t)_{\text{syn}} dt}{\int p(t)_{\text{obs}}^2 dt + \int p(t)_{\text{syn}}^2 dt},$$

where $p(t)_{\text{obs}}$ and $p(t)_{\text{syn}}$ are the observed and synthetic seismograms, respectively. If the synthetic seismogram is null, then $f_2 = 0$, and if the synthetic and observed seismograms are perfectly matched, then $f_2 = 1$; f_2 was calculated by using a time window of 60 sec, starting several seconds before the P -wave arrival time. Estimates of both factors in different frequency ranges provide a quantitative measure of goodness of fit. Combined with the waveform comparison, they give a general picture of the waveform fit between the observed and synthetic ground motions. Variations of the f_1 and f_2 factors with epicentral distance for different frequency ranges are given in Figure 5.

The f_1 values for PGV are shown in Figure 5a. These values suggest that, except for a few sites, our velocity model does a very good job of predicting the peak velocity at sites

in and outside the Seattle basin for all three considered frequency ranges.

The f_1 for the FSA is relatively high at 0.2 Hz (periods of 5 sec), whereas it decreases substantially at frequencies 0.3 and 0.4 Hz, for which the signal energy is small (Fig. 5b). Because most of the energy of the ground motion velocity is carried by waves with a predominant period of about 5 sec and longer, as seen in the waveforms shown in Figures 3 and 4, the value of f_1 at 0.2 Hz is a good representation of the model quality.

Compared to f_1 , goodness-of-fit factor, f_2 , is much more sensitive to the waveform than the amplitude of the motion. Consequently, it can reach values that are much smaller than the f_1 factor for the same sites. The variation of f_2 , shown in Figure 5c, suggests that at many sites where the synthetic and recorded seismograms are not in phase, this factor could be as low as 0.1. Meanwhile, at these sites f_1 could be high. Our model performs reasonably well at matching the north-south and vertical components of motion at most of the sites in the Seattle basin (sites with epicentral distances between 52 and 65 km). At sites outside the basin, f_2 is low. At these sites we match well the amplitude and duration, but not the waveform, of the ground motion.

The goodness-of-fit results demonstrate that in general the large-scale basin structure along the southern edge of the Seattle basin is well represented in our model. Overall, the best fit, in terms of waveform and amplitude, is obtained in the north-south component of the ground-motion velocity, especially at sites in the central part of the basin and with epicentral distances ranging between 52 and 65 km. At these

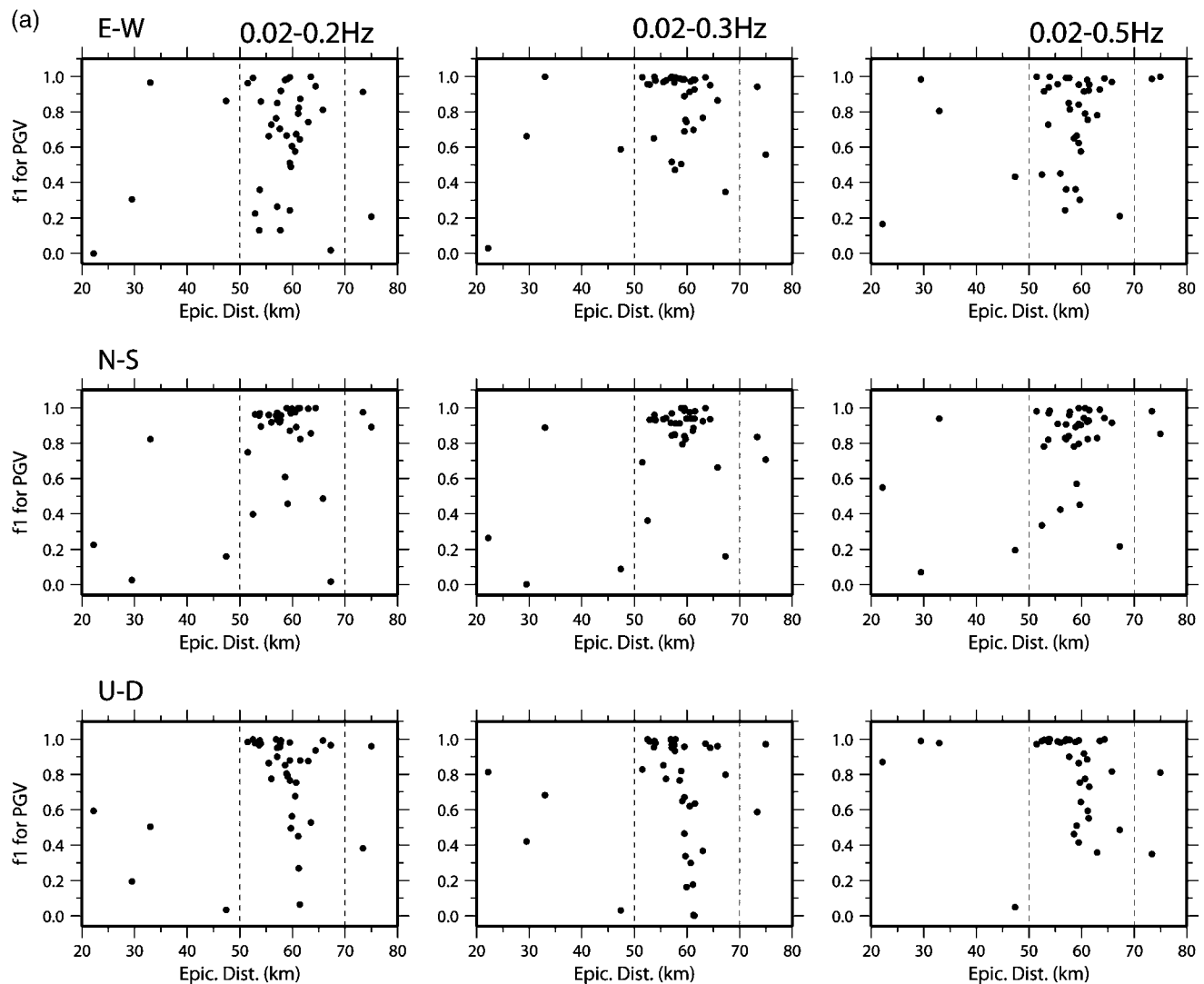


Figure 5. (a) Goodness-of-fit factor, f_1 , for peak ground velocity on east–west, north–south, and up–down components, measured at three frequency ranges: 0.02–0.2 Hz, 0.02–0.3 Hz, and 0.02–0.5 Hz, left, center, and right panels, respectively. The component direction is indicated in the left panels. Vertical dashed lines at 50 and 70 km indicate the epicentral distance of the southern and northern edges of the basin, respectively. *(continued)*

sites the ground motion is dominated by large pulses that correspond to the direct S -waves, basin reflected waves, and basin surface waves generated at the southern edge of the basin.

Discussion

Recent analyses of ground motion from the Nisqually earthquake and other seismic events recorded in the Seattle region reveal the significant effect of the shallow and deep geological structure in increasing the amplitude and duration of ground motion in the Seattle basin. Among the many results of such analyses, two have direct implications for the ongoing process of refinement and validation of 3D velocity models of the Seattle area. The first is that in the Seattle

basin the basin surface waves affected by the deep-basin geometry dominate the ground motion, especially at frequencies lower than 1 Hz (e.g., Pitarka *et al.*, 1999; Frankel *et al.*, 2002; Carver *et al.*, 2002). The second is that there is a clear correlation between variations in site response and Quaternary deposits (Troost *et al.*, 2002; Hartzell *et al.*, 2000; Pratt *et al.*, 2003), especially at frequencies higher than 0.5 Hz.

In this section we show results of analyses of the effects of deep versus shallow geological structure on the ground motion, based on our modeling of ground motion recorded in the Seattle basin. Because the period range used in our simulation is between 2 and 10 sec, our analyses are focused on long-period, basin-structure effects.

Figure 6 shows the distribution of calculated peak

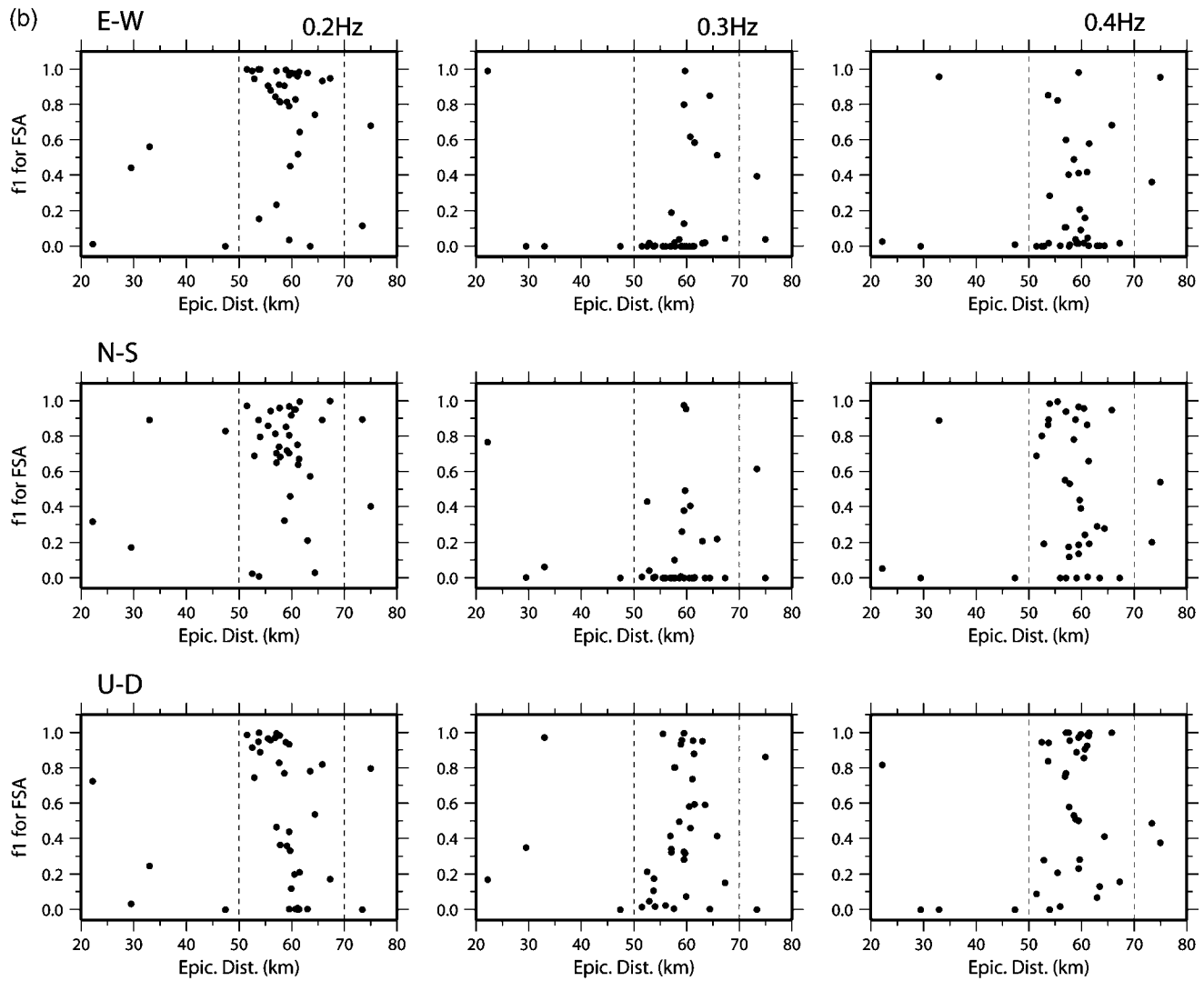


Figure 5. (continued) (b) Goodness-of-fit factor, f_1 , for Fourier amplitude spectrum of the velocity calculated at 0.2 Hz, 0.3 Hz, and 0.4 Hz, left, center, and right panels, respectively. The component direction is indicated in the left panels. Vertical dashed lines at 50 and 70 km indicate the epicentral distances of the southern and northern edges of the basin, respectively. (continued)

ground velocity in the east–west, north–south, and vertical components of motion. In this figure we also show contour lines of the thickness of the unconsolidated sedimentary layer. The peak-velocity distribution indicates that the peak-velocity-amplification pattern is very complex and does not fully coincide with the thickness of the unconsolidated sedimentary layer, especially in the Seattle basin. In this basin the peak-velocity amplification is very different between the two horizontal components. The east–west component of the ground motion is strongly amplified only along the southern edge and in a small area of the central part of the basin, whereas the zone of amplification of the north–south component covers a large part of the basin, offset from the southern basin edge. In general the lateral extension of these zones of peak-velocity amplification correlate with basins and the

thickness of the unconsolidated deposits. This indicates that the long-period waves are affected by the deep and shallow geological structure of the basin as well.

Based on the peak-velocity distribution, there is striking evidence of very large amplification of the ground motion in the north–south direction in both the Seattle and Tacoma basins. In the Seattle basin the north–south component is dominated by surface waves generated at the southern edge of the basin along a zone of strong velocity contrast. The north–south component, which roughly corresponds to the radial component of motion, may also contain Rayleigh waves that were generated in the Tacoma basin and then channeled through the Seattle uplift into the Seattle basin without being scattered (e.g., Pitarka and Irikura, 1996). Our simulation suggests that the amplification pattern is due to

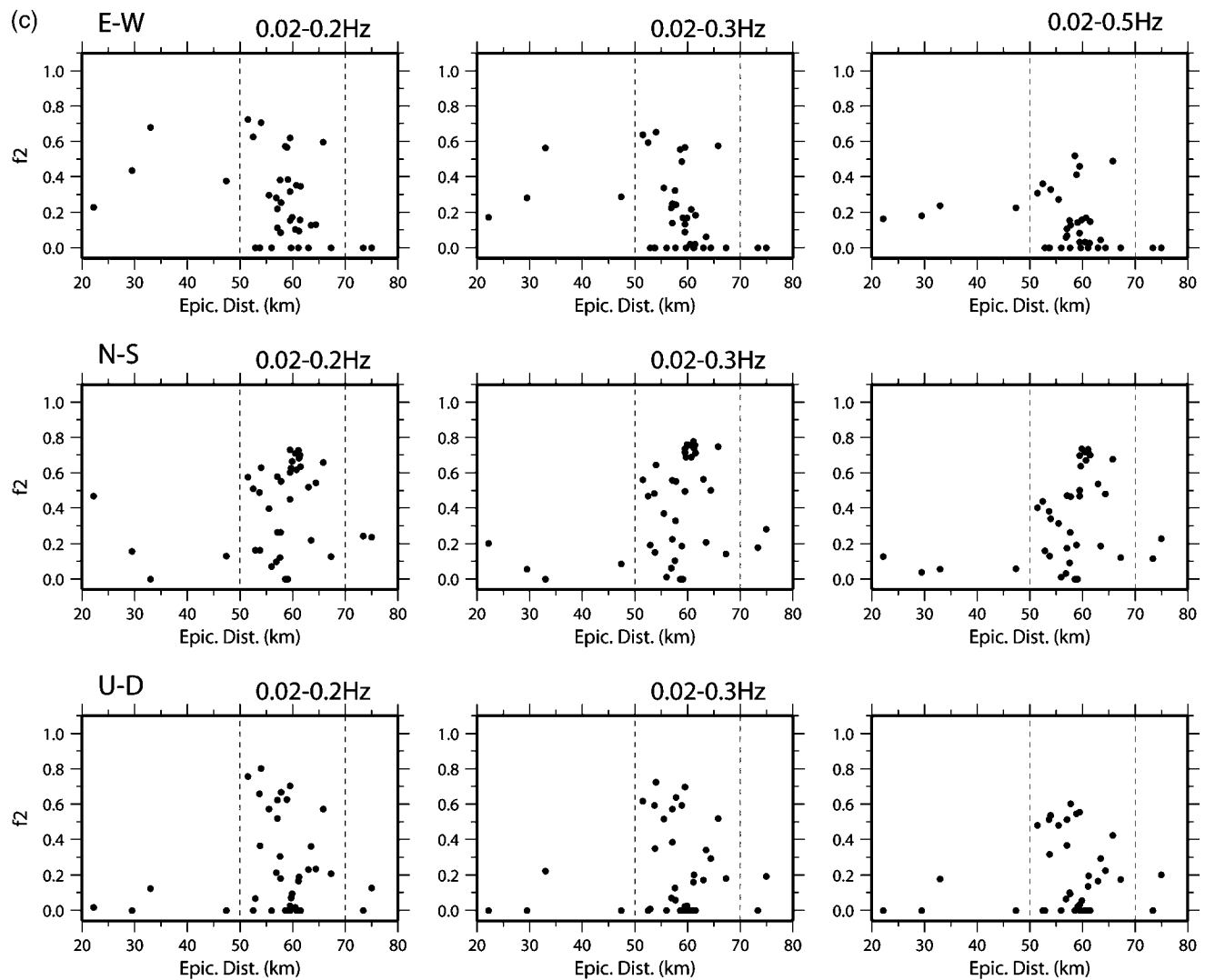


Figure 5. (continued) (c) Goodness-of-fit factor, f_2 , for velocity ground-motion seismograms along east-west, north-south, and up-down directions, bandpass filtered at three frequency bands of 0.02–0.2 Hz, 0.02–0.3 Hz, and 0.02–0.5 Hz, left, center, and right panels, respectively. The component direction is indicated in the left panels. Vertical dashed lines at 50 and 70 km indicate the epicentral distances of the southern and northern edges of the basin, respectively.

3D basin focusing and basin-edge effects. The surface waves remain trapped within the basin sediments. Their constructive superposition may create complex amplification patterns, even at long periods. As discussed previously, the secondary surface waves in the Seattle basin may have been amplified as a result of the thinning of the sedimentary layers toward the north. This structural effect, specific to the Seattle basin, was pointed out by Frankel and Stephenson (2000).

Two recent site-response studies in the Seattle region (Frankel *et al.*, 1999; Hartzell *et al.*, 2000) identified several areas of high amplification in the Seattle basin. These findings, which are based on analyses of ground-motion data at frequencies higher than the ones considered in our study, suggest that the high amplification is due to several factors,

such as 3D basin-edge effects, basin-focusing effects, and higher impedance contrast between the basin sediments and the bedrock. Our modeling results suggest that the 3D basin structure has a strong effect at long periods.

In Figure 7 we show the effect of the unconsolidated sedimentary layer on the ground motion at the Seattle basin sites. In the Seattle basin this layer consists essentially of Quaternary deposits. In this figure we compare Fourier amplitude spectra of recorded (thick line) and synthetic seismograms calculated with the proposed 3D velocity model (thin solid line), and a 3D velocity model without the unconsolidated sedimentary layer (thin dashed line). The panels are aligned following the station epicentral distance, starting with the station closest to the epicenter. The re-

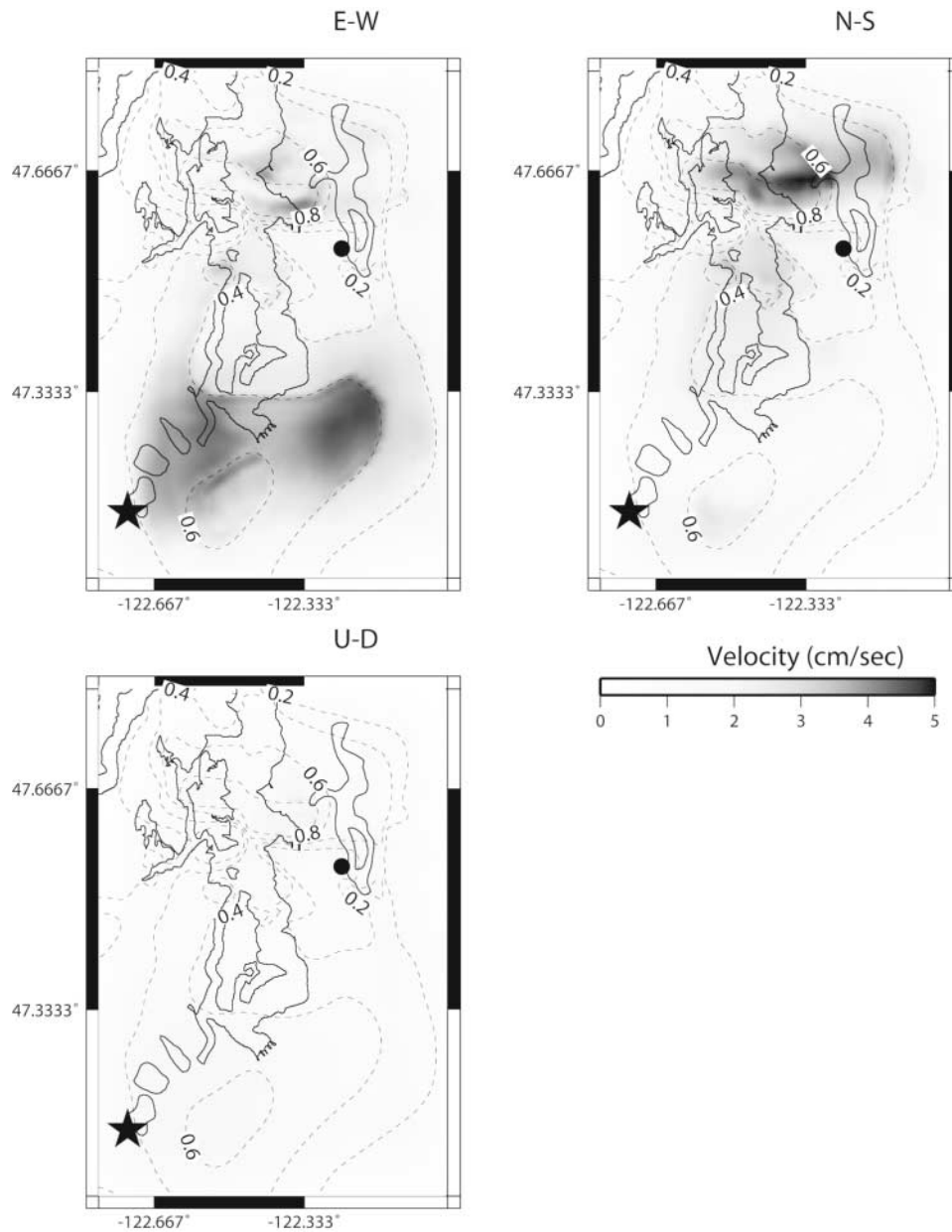


Figure 6. Simulated ground-motion peak velocity for the Nisqually earthquake by using finite-difference seismograms bandpass filtered at 0.02–0.5 Hz. Dashed contour lines show the depth (km) to the base of unconsolidated deposits, and the solid contour line shows the shoreline. Star indicates the epicenter, and the closed circle shows the location of the rock site used as the reference site in estimating the relative amplification of ground motion in the Seattle basin.

corded ground motion at stations close to the basin edge, such as HAR, SDN, KIMB, BHD, and KDK, has a broad spectrum. At these stations the simulation does not match the high-frequency part of the spectrum. In contrast, at deep basin sites the energy is concentrated at frequencies lower than 0.3 Hz, and the comparison between the simulated and recorded spectra is favorable. At these sites the shape of the spectra indicates that the energy associated with frequencies higher than 0.25 Hz is highly attenuated by the basin sedi-

ments. A comparison of results obtained with the two 3D velocity models shows that our representation of the unconsolidated layer in the Seattle basin tends to overamplify the horizontal ground motion around the predominant frequency of 0.18 Hz. The inclusion of this layer in our model causes the broadening of the frequency range of the maximum basin response. This agrees with the observations. As expected, the inclusion of the unconsolidated sedimentary layer improves to some extent the spectral fit at higher frequencies,

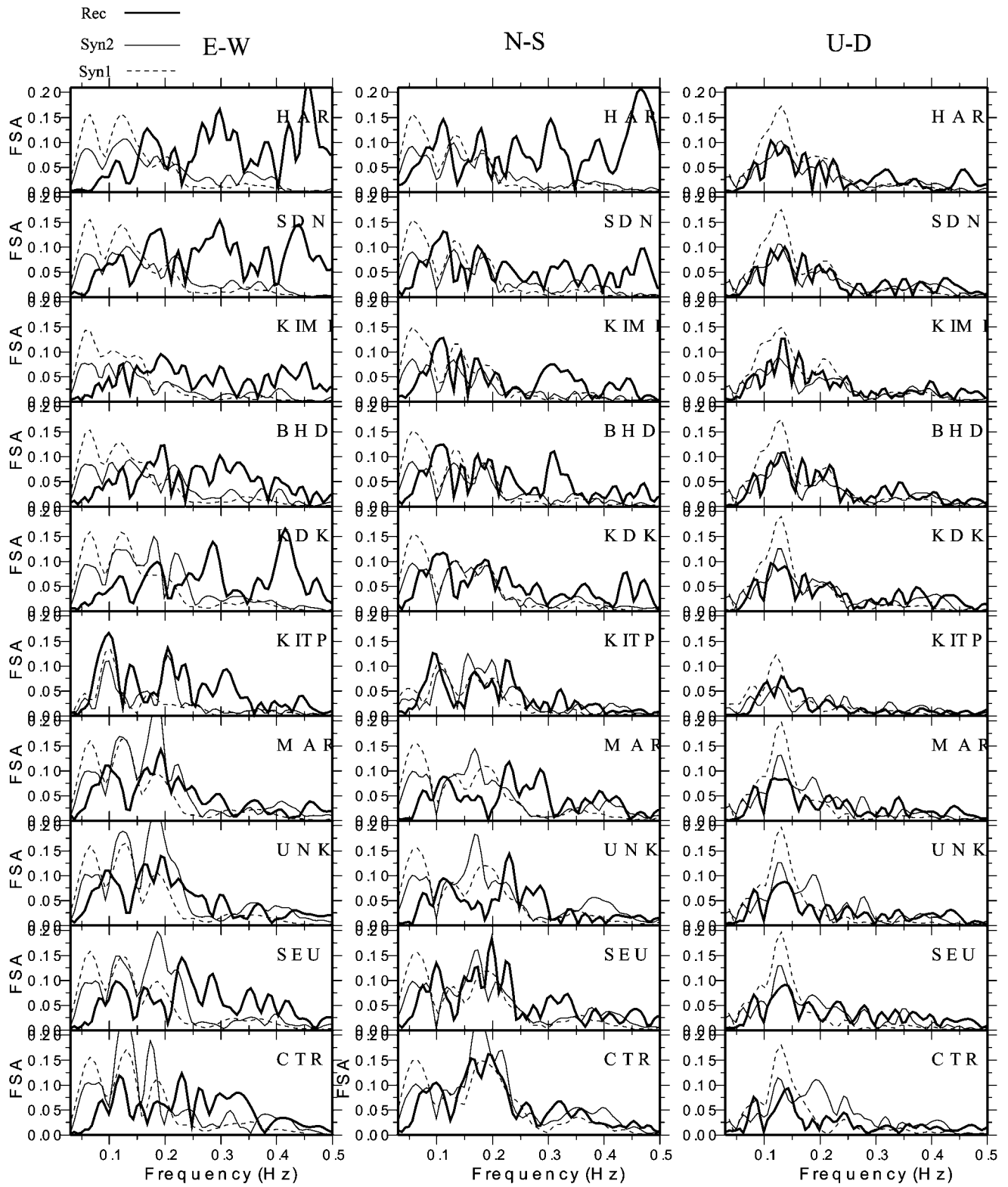


Figure 7. Caption on page 1686.

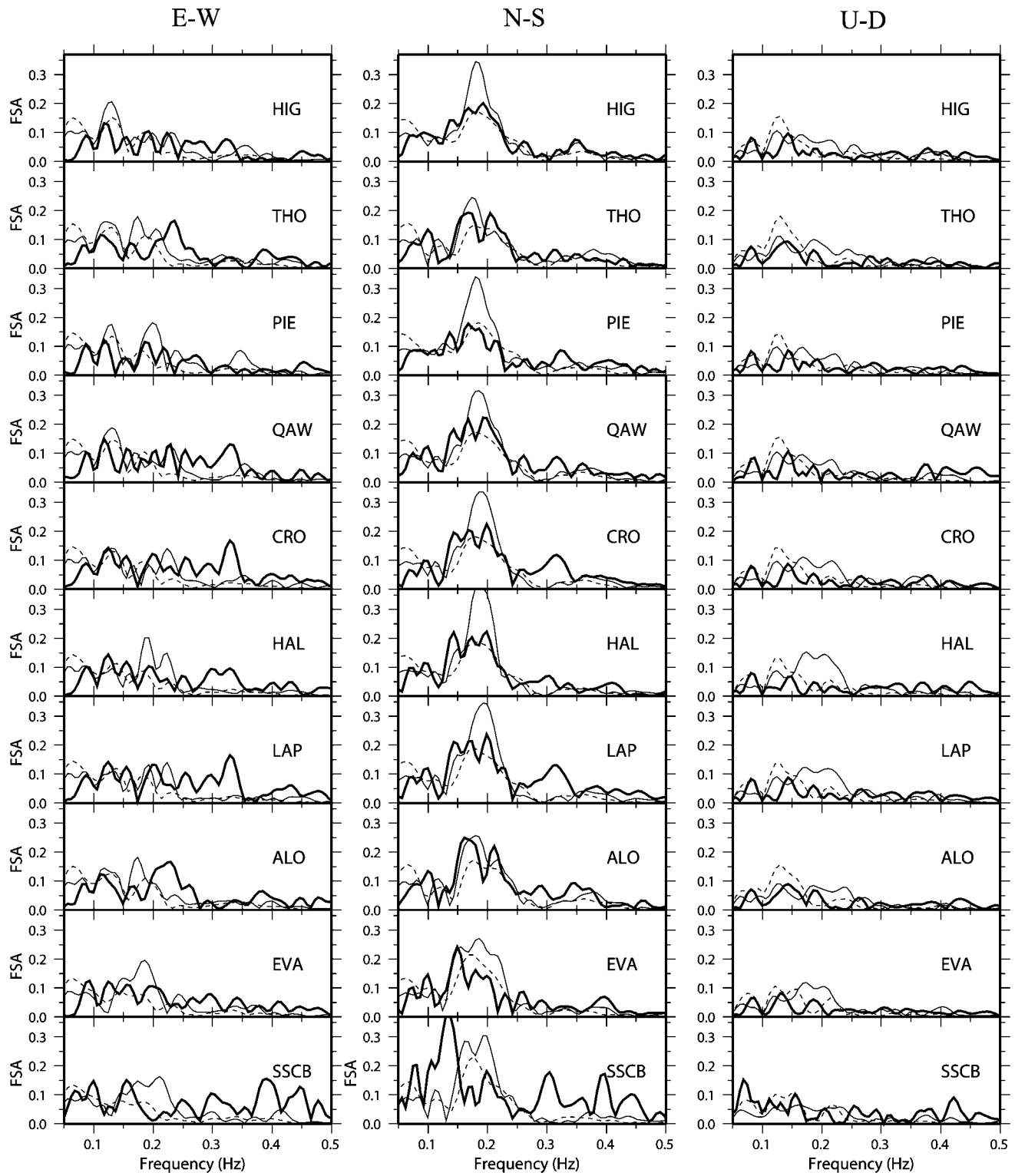


Figure 7. Caption on page 1686.

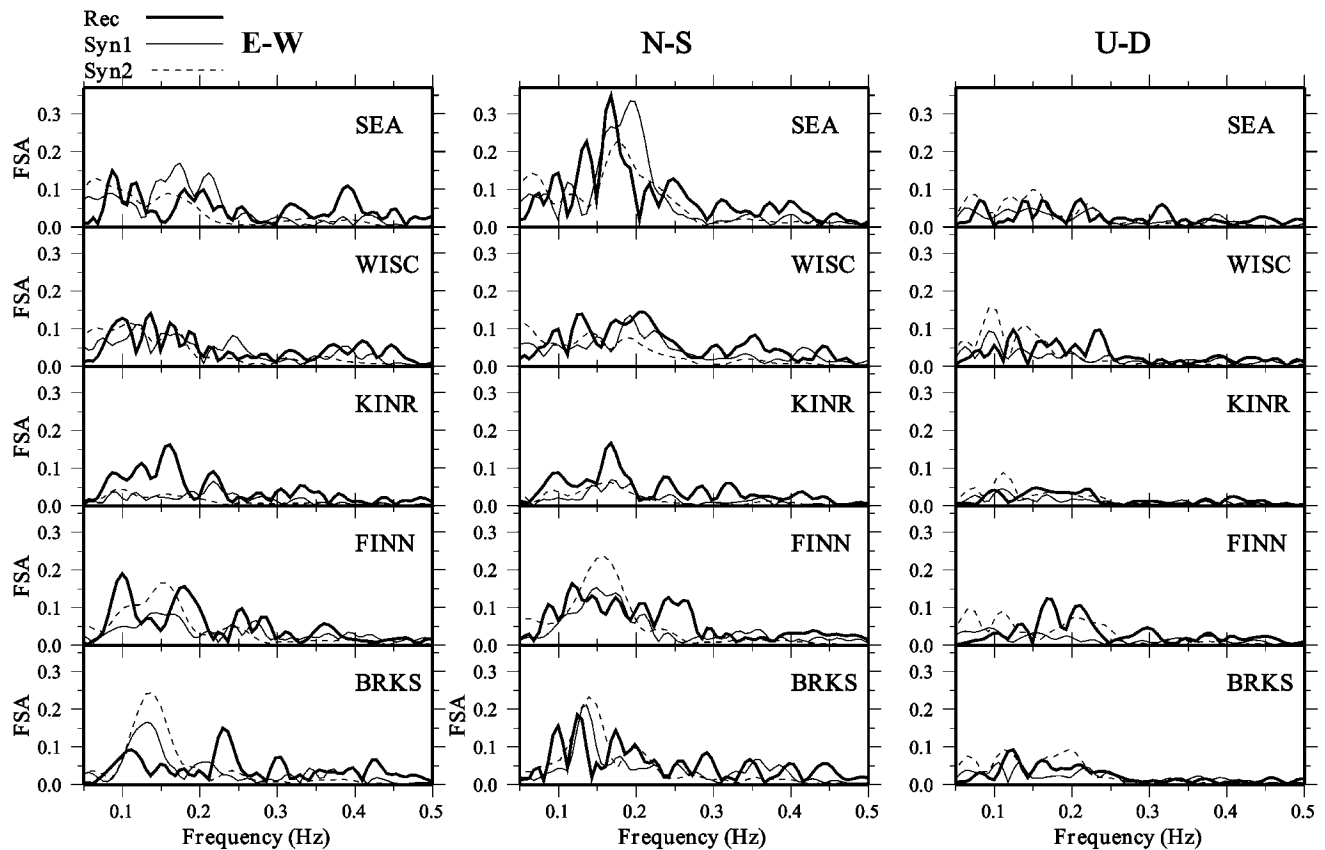


Figure 7. Comparison of Fourier amplitude spectra of recorded (thick line) and synthetic ground-motion velocity computed by using the proposed 3D basin model (thin line), and a modified version of the basin model without the unconsolidated sedimentary layer (dashed line).

too. We recognize that our assumption of representing the unconsolidated deposits by a single layer with a strong velocity contrast may create unrealistic effects, and that a velocity gradient within this layer may yield a better result. Because of the limited computational capacity of the machine available for this study, we were unable to confirm this idea.

The comparison of the simulated and recorded amplitude spectra (see Fig. 7) supports the conclusion that the recorded long-period ground motion in the Seattle basin is strongly affected by the deep basin structure and that the combination of the velocity model of Parsons *et al.* (2001) and the basement geometry of the basin proposed by Blakely *et al.* (1999) do a good job of capturing such effects.

In order to supplement the quality of our 3D model analysis in the Seattle region, we calculated the basin amplification at a linear station array across the Seattle basin (east-west line in Fig. 1a) by using simulated ground motion from the Nisqually earthquake. We compared it with the amplification estimated by Pratt *et al.* (2003) by using ground-motion recordings of the Chi-chi, Taiwan, earthquake. The location of our station array is very close to that of the 1999 SHIPS array that was used by Pratt *et al.* (2003) in their study

of the amplification of seismic waves in the Seattle basin. The first and last stations of our array correspond to stations 1296 and 2570 in their study, respectively. Our stations are equally spaced at 400 m. Following the procedure used by Pratt *et al.* (2003), we estimated the basin amplification at 0.2 and 0.33 Hz by calculating the spectral ratios of the simulated horizontal motion from the Nisqually earthquake relative to a bedrock site. Pratt *et al.* (2003) estimated the basin amplification on the basis of the average of spectral ratios of the recordings of the horizontal motion from the Chi-chi, Taiwan, earthquake relative to the average of two bedrock sites at the west end of the array in the Olympic Mountains. Because these two sites lie outside our 3D model area, we choose a site at -122.25 E, 47.549 N, as a reference (see Fig. 6). This soft-rock site at Seward Park, south of the basin edge, was used as a reference in previous site-response studies of the Seattle area (station SQ1 in Frankel *et al.*, 1999; Hartzell *et al.*, 2000). Based on recordings of the Chi-chi earthquake, Pratt *et al.* (2003) estimated that the site response relative to the Seward Park reference site will be at least about 30% smaller than the site response relative to the Olympic Mountains reference site that was used in their study. We reduced their amplification factors by 30%

in order to obtain the corresponding amplification relative to the Seward Park reference site used in our calculation.

The comparison between the two amplifications at 0.2 Hz and 0.33 Hz relative to the Seward Park reference site is shown in Figure 8. The variation of the basin amplification factor along the considered east–west array is very similar in the two studies. Basically, its shape is similar to the basin basement geometry. Our simulated amplification tends to be larger in the central part of the basin and smaller in the western part of the basin. Although the long-period ground motion from the Nisqually earthquake was generated by a deep source, the simulated long-period ground motion is affected by the radiation pattern. This is not the case for the recorded teleseismic ground motion from the Chi-chi earthquake. Given the completely different nature of the earthquake sources, the similarity between the two basin amplification factors is very encouraging. It demonstrates that features of the overall long-scale basin structure along the east–west direction are adequately presented in the model. Seismological constraints, based on modeling of amplification factors derived from recordings of local and regional earthquakes in the Puget Sound region, will be very helpful in future refinements of proposed 3D velocity models.

Conclusions

In this study we show results of validation analyses of a velocity model for 3D long-period ground-motion simulations in the Puget Sound region. Our simulation of ground motion from the Nisqually earthquake suggests that the regional tomographic velocity model of Parsons *et al.* (2001), combined with the Seattle basin basement geometry proposed by Blakely *et al.* (1999) and the north–south and east–west basin-structure cross sections from the SHIPS experiments, provide very good information that is essential for developing efficient velocity models of the Seattle region for 3D simulations. Our velocity model performs well in reproducing basin structural effects on long-period ground motion from the Nisqually earthquake in the Seattle basin. The analyses of our simulation results indicate that waves with periods longer than 3 sec are mainly affected by the deep geological structure of the Seattle basin. We found that the Quaternary deposits also affect the ground motion at long periods. Their representation in our velocity model by a single layer with a strong velocity contrast is not adequate, especially in the southern part of the model. As pointed out by Frankel and Stephenson (2000), future improvements of the velocity models for 3D simulations need to be focused

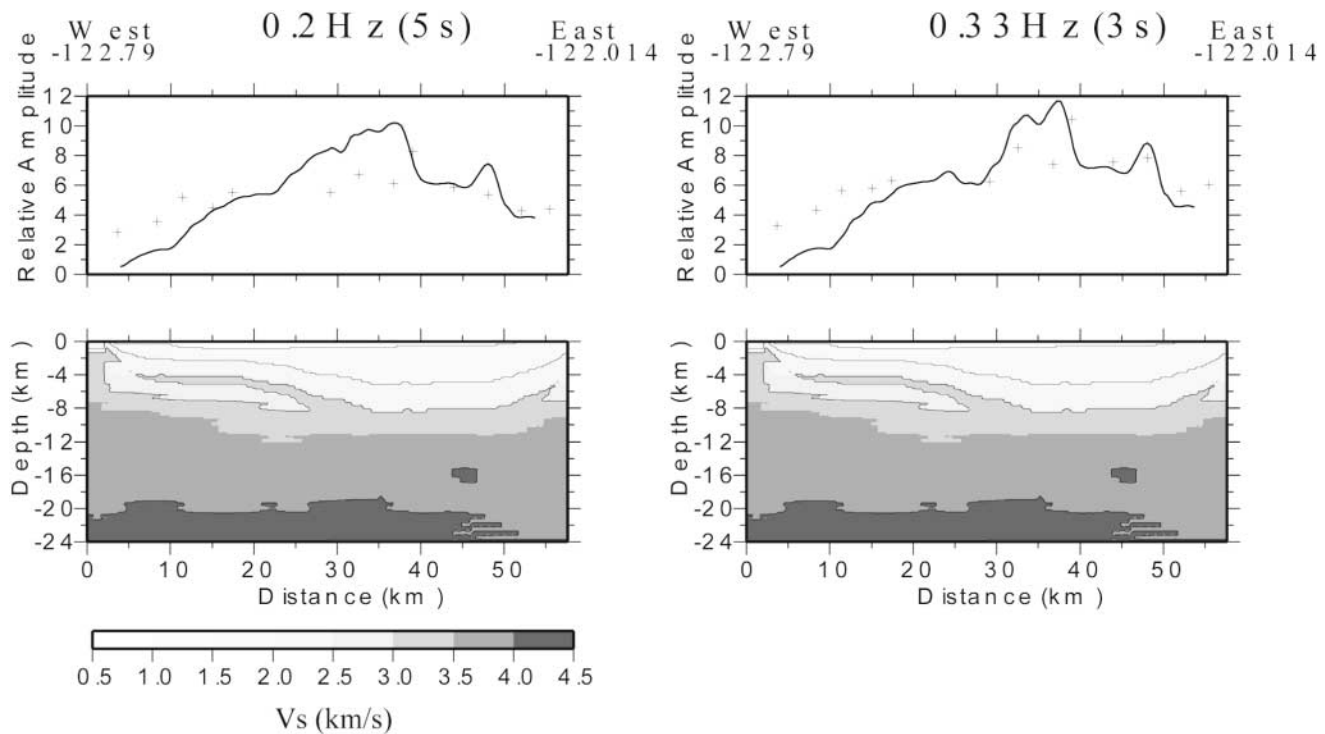


Figure 8. Spectral amplitudes relative to a rock site indicated in Figure 6, calculated at specific frequencies shown at the top of each panel. Top panels: comparison of relative spectral amplitudes by using synthetic seismograms from the Nisqually earthquake (solid line) and recorded ground motion from the Chi-chi, Taiwan, earthquake (crosses) (Pratt *et al.*, 2003) along the east–west line shown in Figure 1. Bottom panels: Top 24 km of the vertical cross section of the 3D velocity model along the east–west line.

on the shallow structure of the basins in the Puget Sound region. These improvements should be guided by modeling observed ground-motion data for several seismic sources at periods shorter than 2 sec (e.g., Pratt *et al.*, 2003). Model refinements in the Seattle region, using seismological constraints derived from this study and simulations of recorded ground motion from several seismic events, are the subject of another ongoing study.

Our velocity model is given on a regular grid and is available upon request.

Acknowledgments

This study is supported by the U.S. Geological Survey (USGS), Department of the Interior, under USGS Award Number 02-HQ-GR-0049. We thank Tom Parsons and Tom Brocher for providing their tomographic model of the Puget Sound area as well as information about related publications on the SHIPS experiment. We thank Tom Pratt for providing his amplification profile across the Seattle basin, and Samuel Johnson for providing his model of the thickness of the Quaternary layer in the Seattle region. The help of Susan Rhea, who prepared the data in a format suitable for our codes, is appreciated. The suggestions made by Tom Brocher and two anonymous reviewers were very helpful and are much appreciated. Figures were prepared by using the G.M.T. graphics program of Smith and Wessel.

References

- Blakely, R. J., R. E. Wells, and C. S. Weaver (1999). Puget Sound aeromagnetic maps and data, *U.S. Geol. Surv. Open-File Rept.* 99-514, <http://geopubs.wr.usgs.gov/open-file/of99-514>.
- Brocher, T. M., and L. A. Ruebel (1998). Compilation of 29 sonic and density logs from 23 oil test wells in western Washington state, *U.S. Geol. Surv. Open-File Rept.* 98-249, 41 pp.
- Brocher, T. M., T. Parsons, K. C. Creager, R. S. Crosson, N. P. Symons, G. Spence, B. C. Zelt, P. T. C. Hammer, R. D. Hyndman, D. C. Mosher, A. M. Trehu, K. C. Miller, U. S. ten Brink, M. A. Fisher, T. L. Pratt, M. G. Alvarez, B. C. Beaudoin, and C. S. Weaver (1999). Wide-angle seismic recordings from the 1998 Seismic Hazards Investigation in Puget Sound (SHIPS), western Washington and British Columbia, *U.S. Geol. Surv. Open-File Rept.* 99-314, 110 pp.
- Brocher, T. M., T. Parsons, R. J. Blakely, N. I. Christensen, M. A. Fisher, R. E. Wells, and SHIPS Working Group (2001). Upper crustal structure in Puget Lowland, Washington: results from the 1998 Seismic Hazards Investigation in Puget Sound, *J. Geophys. Res.* **106**, 13,541–13,564.
- Brocher, T. M., T. Parsons, A. M. Trehu, C. M. Snelson, and M. A. Fisher (2003). Seismic evidence for widespread serpentinized forearc upper mantle along the Cascadia margin, *Geology* **31**, 267–270.
- Calvert, A. J., M. A. Fisher, and SHIPS Working Group (2001). Imaging the Seattle fault zone with high-resolution seismic tomography, *Geophys. Res. Lett.* **28**, 2337–2340.
- Carver, D., A. Frankel, and T. Bice (2002). Seattle urban array records of the 28 February 2001, M 6.8 Nisqually earthquake and its aftershocks, *Seism. Res. Lett.* **73**, 266.
- Crosson, R. S. (1976). Crustal structure modeling of earthquake data. Velocity structure of the Puget Sound region, Washington, *J. Geophys. Res.* **81**, 3047–3054.
- Finn, C. A., W. M. Philips, and D. L. Williams (1991). Gravity anomaly and terrain maps of Washington. U.S. Geol. Surv. Geophys. Invest. Map GP-988.
- Frankel, A., and W. Stephenson (2000). Three-dimensional simulations of ground motions in the Seattle region for earthquakes in the Seattle fault zone, *Bull. Seism. Soc. Am.* **90**, 1251–1267.
- Frankel, A., D. Carver, E. Cranswick, M. Meremonte, T. Bice, and D. Overturf (1999). Site response for Seattle and source parameters of earthquakes in the Puget Sound region, *Bull. Seism. Soc. Am.* **89**, 468–483.
- Frankel, A., D. Carver, and R. A. Williams (2002). Nonlinear and linear site response and basin effects in Seattle for the M 6.8 Nisqually, Washington, earthquake. *Bull. Seism. Soc. Am.* **92**, 2090–2109.
- Graves, R. W. (1996). Simulating seismic wave propagation in 3D elastic media using staggered-grid finite differences, *Bull. Seism. Soc. Am.* **86**, 1091–1106.
- Hall, J. B. and K. L. Othberg (1974). Thickness of unconsolidated sediments, Puget Lowland, Washington. State of Washington, Department of Natural Resources, Geologic Map GM-12.
- Hartzell, S., D. Carver, E. Cranswick, and A. Frankel (2000). Variability of site response in Seattle, Washington, *Bull. Seism. Soc. Am.* **90**, 1237–1250.
- Ichinose, G. A., H. K. Thio, and P. G. Somerville (2004). Rupture process and near-source shaking of the 1965 Seattle–Tacoma and 2001 Nisqually intraslab earthquakes. *Geophys. Res. Lett.* **31**, L1064, doi 10.1029/2004G1019668.
- Johnson, S. Y., S. V. Dadisman, J. Childs, and W. D. Stanley (1999). Active tectonics of the Seattle Fault and cross-cutting strike-slip faults in the central Puget Sound Lowlands, Washington: implications for earthquake hazards, *Geol. Soc. Am. Bull.* 1042–1053.
- Miller, K. C., and C. M. Snelson (2001). Structure and geometry of the Seattle basin, Washington state—results from Dry SHIPS '99: Collaborative research (USGS, OSU, UTEP), Progress Report to U.S. Geological Survey.
- Parsons, T., R. J. Blakely, and T. M. Brocher (2001). A simple algorithm for sequentially incorporating gravity observations in seismic travel-time tomography, *Int. Geol. Rev.* **43**, 1073–1086.
- Pitarka, A. (1999). 3D elastic finite-difference modeling of seismic wave propagation using staggered grid with non-uniform spacing, *Bull. Seism. Soc. Am.* **89**, 54–68.
- Pitarka, A., and K. Irikura (1996). Basin structure effects on long period strong motions in the San Fernando valley and the Los Angeles Basin from the 1994 Northridge earthquake and an aftershock, *Bull. Seism. Soc. Am.* **86**, S126–S137.
- Pitarka, A., N. F. Smith, R. W. Graves, and P. G. Somerville (1999). Modeling the effect of the Puget basin on strong motions from earthquakes on the Seattle fault, *Seism. Res. Lett.* SSA Meeting Abstr., 220.
- Pratt, T. L., S. Johnson, C. Potter, W. Stephenson, and C. Finn (1997). Seismic reflection images beneath Puget Sound, western Washington state: the Puget Lowland thrust sheet hypothesis, *J. Geophys. Res.* **102**, 27,469–27,489.
- Pratt, T. L., T. M. Brocher, C. S. Weaver, K. C. Creager, C. M. Snelson, R. S. Crosson, K. C. Miller, and A. M. Trehu (2003). Amplification of seismic waves by the Seattle basin, Washington state, *Bull. Seism. Soc. Am.* **93**, 533–545.
- Silva, W. J., I. G. Wong, and R. B. Darragh (1995). Engineering characterization of earthquake strong ground motions in the Pacific Northwest, in *Assessing Earthquake Hazards and Reducing Risk in the Pacific Northwest*, U.S. Geol. Surv. Profess. Pap. 1560.
- Troost, K. G., D. B. Booth, and S. A. Simel (2002). Geologic controls on site response and ground failures in Seattle during the 2001 Nisqually earthquake, *Seism. Res. Lett.* **73**, 214.
- Van Wagoner, T. M., R. S. Crosson, K. C. Creager, G. Medema, L. A. Preston, N. P. Symons, and T. M. Brocher (2002). Crustal structure and relocated earthquakes in the Puget Lowland, Washington, from high-resolution seismic tomography, *J. Geophys. Res.* **107**, no. B12, 2831, doi 10.1029/2001JB000710.
- Williams, R. A., W. J. Stephenson, A. D. Frankel, and J. K. Odum (1999). Surface seismic measurements of near-surface P- and S-wave seismic velocities at earthquake recording stations, Seattle Washington, *Earthquake Spectra* **15**, 565–584.
- Wong, I., J. Bott, W. Silva, D. Anderson, M. Mabey, B. Metcalfe, S. Olig, A. Sanford, K. Lin, D. Wright, A. Sparks, and A. Sojourner (1998).

Microzoning for earthquake ground shaking in three urban areas in the Western United States. Presented at Sixth U.S. National Conference on Earthquake Engineering, June 1998, Seattle, Washington.

Yount, J. C., G. R. Dembroff, and G. R. Barats (1985). Map showing depth to bedrock in the Seattle 30' by 60' quadrangle, Washington. *U.S. Geol. Surv. Mis. Field Studies Map MF-1692*, scale 1:100,000.

URS Corporation
566 El Dorado Street
Pasadena, California 91101
arben_pitarka@urscorp.com

Manuscript received 20 August 2003.